Progress Report 2: Incorporating Alternative Modes of Innate Immunity

Avril Wang

September 13th, 2021

Introduction

1. Immunity is an important modulator of malaria intra-host dynamics.
    - Both innate immunity and adaptive immunity are needed to control parasite population during peak parasitemia [4].
    - Adaptive immunity is also needed for infection resolution [5].
2. Innate immunity affect parasite dynamics via two routes: indiscriminate red blood cell (RBC) removal and targeted infected RBC removal.
    - Indiscriminant RBC removal entails higher rate of general RBC destruction during the infection phase, which leads to host anemia and impedes parasite reproduction by limiting food supply [6].
    - Indeed, the majority of RBC loss incurred during a malaria infection is ascribed to indiscriminate RBC removal rather than parasitism [6].
    - Targeted infected RBC removal represents a more precise parasite clearing mechanism and is important to prevent infection recrudescence [6].
3. Given the importance of host immune response on parasite and RBC population, I have been working on incorporating different innate immunity models into our intra-host model. Each innate immunity model differs in their assumption of immunity magnitude, mode of immunity activation, and mode of immunity maintenance.
4. Immunity aside, I have also worked on other aspect of modelling, which includes:
    - Examining the effects spline transformation on optimization results.
    - Examining the effects of cue range and degrees of freedom (spline function) on optimization results.
    - Constructing an alternative model that abides by the canonical next cycle conversion route.
    - Thinking of methods to more effectively simulate strategy competition for co-infection.

Progress

0.1 Replicating Greischar's saturating immunity model

Dr. Greischar generously provided me with her code. With reference to her immunity function, I was able to replicate her result when optimizing time-based conversion rate strategy (Figure 1).

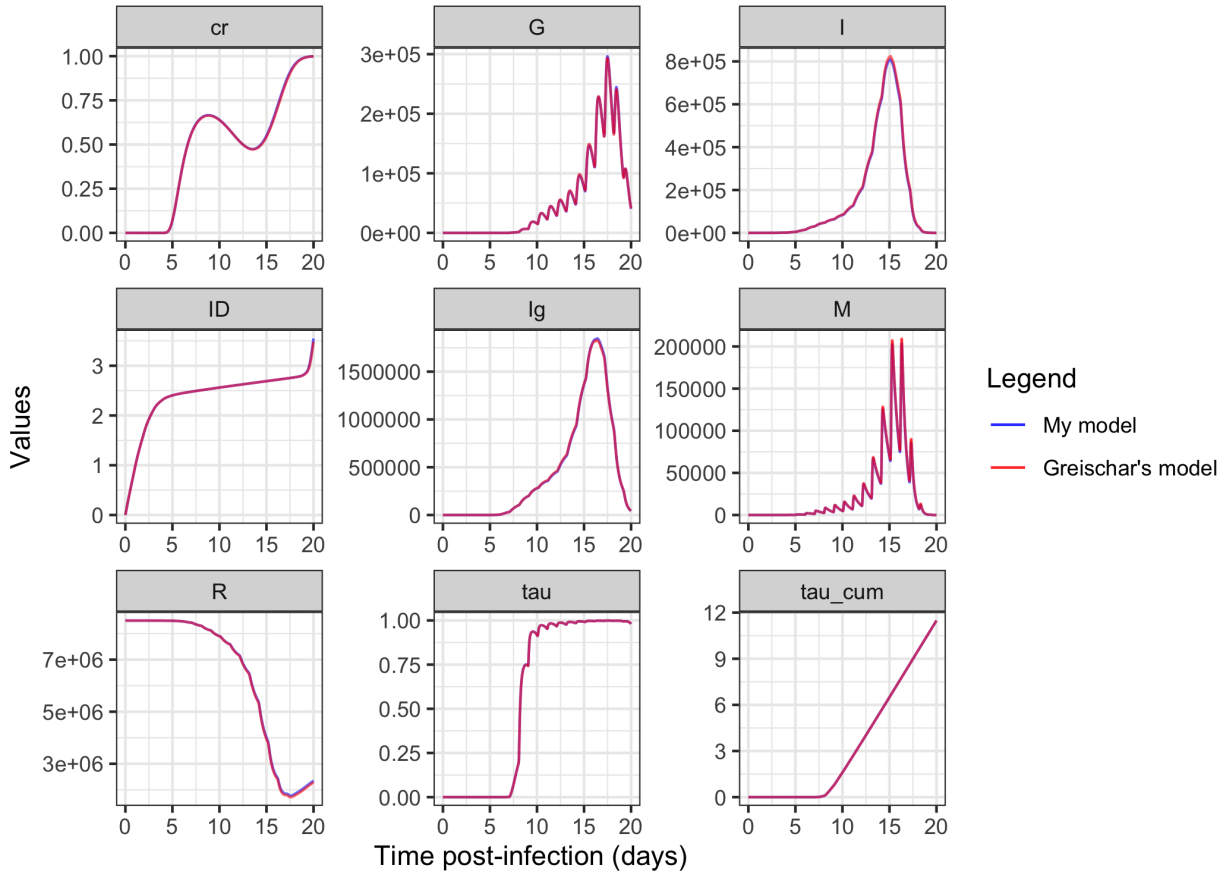

Figure 1: Successful replication of Greischar *et al.*'s result for saturated immunity model. Infection dynamics for my own code (blue) is plotted together with Greischar's optimal conversion strategy (red).

0.2 Next cycle conversion model

All subsequent models are performed using the new iterations of the intra-host model (Figure 2; Appendix), which introduces a lag between conversion rate decision and production of merozoite/gametocyte (herein referred to as the lag model). In the original Greischar model, conversion rate decision is made during merozoite invasion and the infected RBC is immediately committed to either the asexual route or sexual route. In reality, the majority of malaria infection cycle follows the next cycle conversion route where conversion rate decision results in the production of either sexually-committed merozoite that produces sexually-committed infected RBC upon invasion or asexual merozoite that will continue the asexual cycle (same cycle conversion exists, but its significance in infection is unknown) [1].

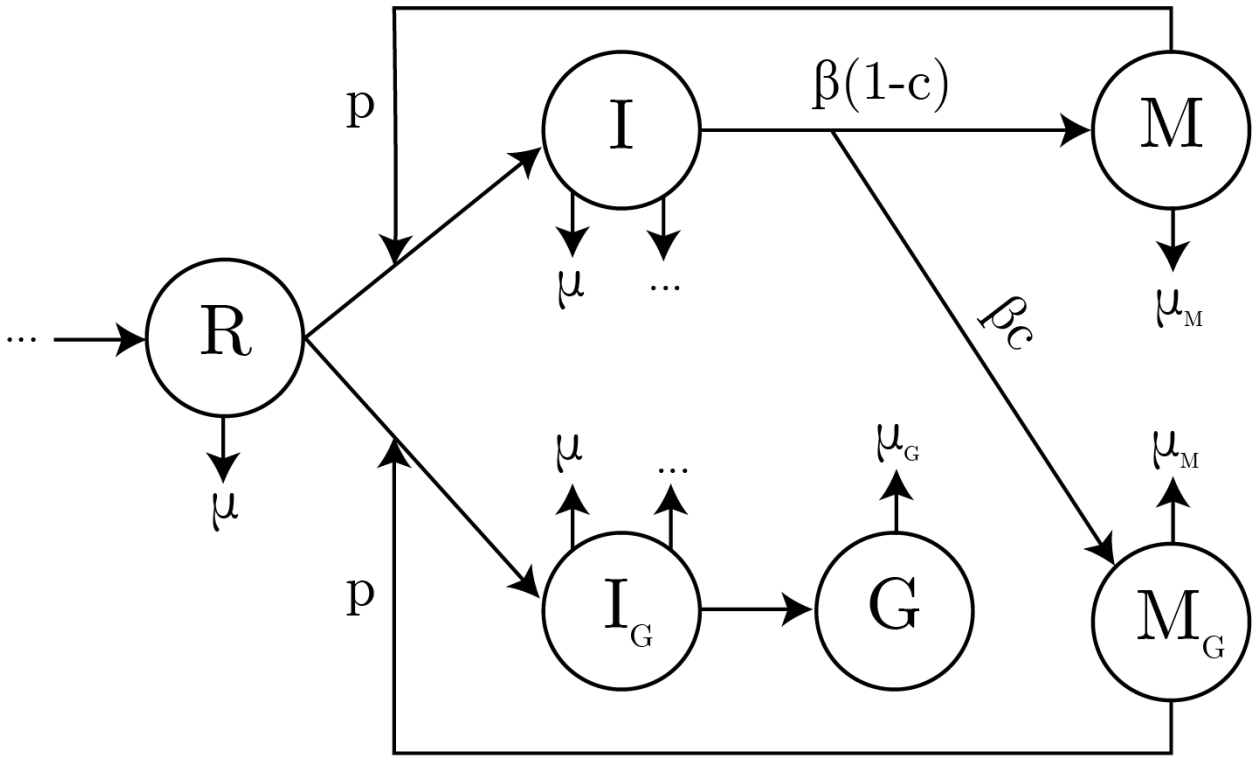

Figure 2: Flow diagram of new model that incorporates next cycle conversion. R is the density of susceptible RBC, I is the density of asexually-committed infected RBC, I_G is the density of sexually-committed infected RBC, M is the density of asexually-committed merozoite, M_G is the density of sexually-committed merozoite, and G is the density of gametocyte. " ..." represents either RBC renewable expression (differs depending on model) or immune removal of infected RBC.

When the model is optimized using time-based conversion rate strategy, as expected, there is little change in overall infection dynamics (Figure 3A). Here, the lag between conversion rate decision and merozoite/gametocyte production does not decrease overall parasite fitness given that conversion rate is based on the predictable flow of time rather than the unpredictable cue. When conversion rate is cue-dependent (e.g. asexual infected RBC density), parasites tend to have lower fitness in our lag model compared to the original model (Figure 3B). In the lag model, parasites have to commit to the asexual/sexual route one day ahead of time (the period it takes for infected RBC to mature and produce merozoite), which meant that optimal conversion rate strategy is likely limited by the unpredictability of future host condition.

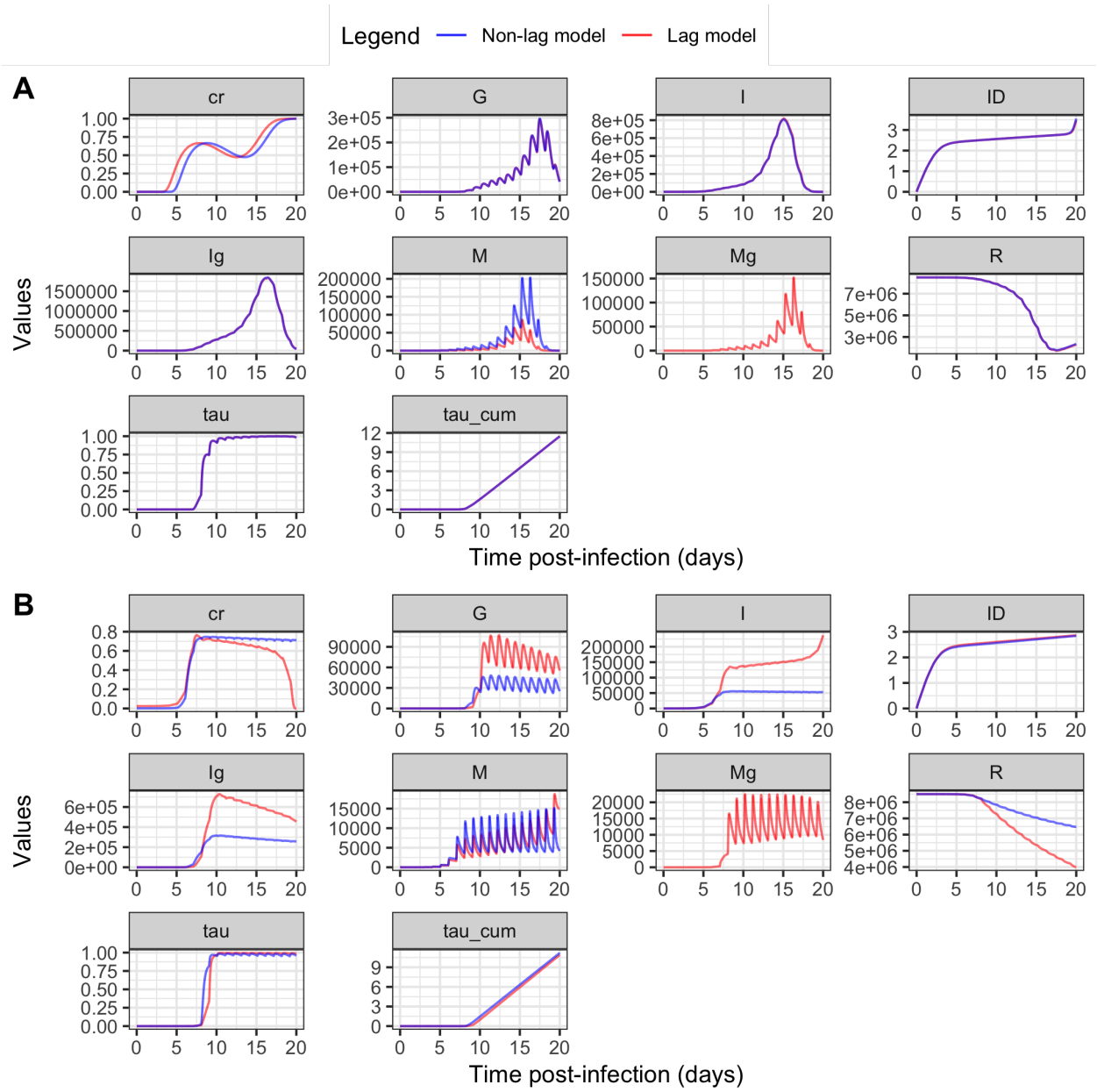

Figure 3: Next cycle conversion alters infection dynamics if conversion rate is cue-dependent. (A) represents the optimal conversion rate strategy when conversion rate is dependent on time. While the lag model exhibits an earlier increase in conversion rate, parasite and RBC population dynamics is similar between the lag and non-lag model. (B) represents the optimal conversion rate strategy when conversion rate is dependent on asexual infected RBC density $I(t)$. The lag model predicts higher infected RBC and gametocyte density than the non-lag model. Infected RBC density range is bounded from 0 to $2.18 * 10^6$. All infections are simulated assuming saturating immunity.

0.3 Three modes of innate immunity

The original Greischar model incorporated a model of innate immunity that removes infected RBCs and saturates with parasite density. Immunity action is represented by $\frac{a}{b+I(t)}$ where $a = 150$ and $b = 100$. To

explore other forms of innate immunity, I incorporated two other immunity modes, one adopted from Kochin *et al.* [3] and the other from Kamiya *et al.* [2]. Kochin's model of innate immunity explicitly models effector cell population and only considers targeted infected RBC removal.

$$\frac{dE}{dt} = \sigma I(t)(1 - E(t)) - \mu_E E(t)$$

Where $E(t)$ represent the density of the effector cells that has a σ chance of becoming activated when they interact with an infected RBC $I(t)$. μ_E is the decay rate for innate immunity. Infected RBCs are removed when they interact with the effector cells such that

$$\frac{dI}{dt} = ... - \gamma E(t) I(t).$$

Where ... represent the dynamics of infected RBCs due to RBC bursting and natural death and γ represents the rate of immune clearance of infected RBC. σ was set to $1.17 * 10^{-8}$, μ_E was set to 0.3, and γ was set to 133.

I also adopted Kamiya's model for innate immunity, which considers both targeted infected RBC removal and indiscriminate RBC removal. Here, the magnitude of immune response is scaled proportionally to the activation constant and $\frac{I(t)+I_G(t)}{I_{max}}$ where I_{max} is the maximum infected RBC reachable in a "typical" infection $(2.18 * 10^6)$. Here, I assumed that sexually-committed RBCs also elicit immune response and is removed targeted immune response, but that is debatable. The dynamics of targeted infected RBC removal $W(t)$ and indiscriminate RBC removal $N(t)$ is as follows:

$$\frac{dW}{dt} = \psi_W \frac{I(t) + I_G(t)}{I_{max}}(1 - W(t)) - \frac{W(t)}{\phi_W}$$

$$\frac{dN}{dt} = \psi_N \frac{I(t) + I_G(t)}{I_{max}}(1 - N(t)) - \frac{N(t)}{\phi_N}$$

where ψ_W and ψ_N are activation constants and ϕ_W and ϕ_N are decay rates. All parameters are set to the values obtained for 10^4 inoculation dosage. Infected RBCs are removed via

$$\frac{dI}{dt} = ... - (-ln(1 - N(t) - ln(1 - W(t))I(t).$$

An alternative form of RBC replenishment is also included, but I will not outline it in this report.

I repeated the optimization process for time-based and asexually-infected RBC conversion rate for all three models (Figure 4). Overall, different modes of innate immunity significantly affected infection dynamics. Both Kochin's and Kamiya's innate immunity model resulted in lower infected RBC, merozoite, and gametocyte density (Figure 4) with Kamiya's model resulting in the lowest parasite density. When optimizing time-based conversion strategy, adopting Kochin's and Kamiya's models of innate immunity resulted in earlier increase in conversion rate (Figure 4A). A similar trend was observed with infected RBC-based conversion rate strategy with Kochin's model of innate immunity (Figure 4B). Overall, cue-dependent conversion rate strategy seem to be more sensitive to changes in innate immunity modes, possibly due to the fact that infected RBC density leads to consistently higher parasite removal rate in both Kochin's and Kamiya's innate immunity models which increases the benefit of adopting a high conversion rate.

None of the current result with cue-dependent conversion rate strategy should be taken seriously. More tests have to be ran with the effects of cue range. Additionally, a more realistic cue for infected RBC would be all infected RBC, rather than just those that are asexually-committed.

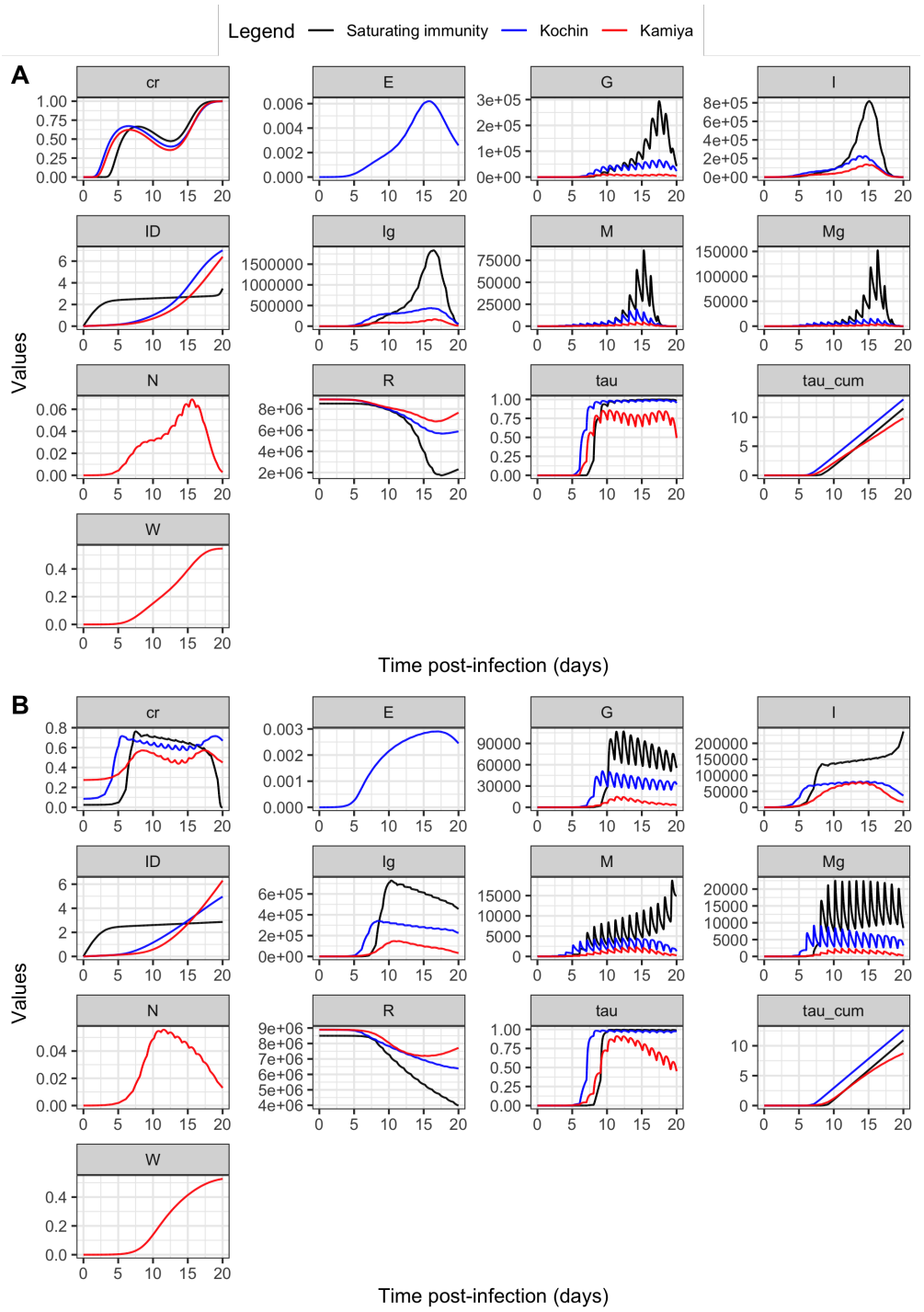

Figure 4: Choice of innate immunity model signficantly affects cue-dependent conversion rate strategy. (A) represents the optimal conversion rate strategy when conversion rate is dependent on time. (B) represents the optimal conversion rate strategy when conversion rate is dependent on asexual infected RBC density $I(t)$ bounded from 0 to $2.18 * 10^6$. All infections are simulated assuming saturating immunity.

0.4 Effects of spline transformation methods, cue range, degrees of freedom, and optimization methods

Before delving into more serious modelling, I wanted to ensure that none of our optimal conversion rate strategy is constrained by spline transformation methods, cue range, degrees of freedom, and optimization methods.

Currently, all conversion rate functions are double-exponentiated (e^{-e^c}) to limit conversion rate between 0 and 1. Here, I tested the effects of other methods of spline transformation, including normalization ($\frac{c-min(c)}{max(c)-min(c)}$) and logistic transformation ($\frac{1}{1+e^{-c}}$). The range at which a particular cue is optimized (cue range) and the degrees of freedom of the spline function (which dictates number of internal knots) dictate the complexity of conversion rate strategy. Here, I investigated the effects of shorter and longer cue ranges and higher degrees of freedom. Lastly, all previous optimization attempts were performed using L-BFGS-B algorithm, which is a gradient-based local optimization algorithm. Here, I tested out whether using global optimization methods such as particle swarm optimization (PSO) and genetics algorithm (GA) affected optimization results. All modelling is performed using saturating immunity with asexually infected RBC (0 to $2.18 * 10^6$ as default range) as the cue.

Conversion rate transformation alters the optimal conversion rate strategy found, with normalization transformation producing the strategy with the lowest fitness (Figure 5A; Fig 5E). Overly wide cue range also decreases our ability to locate the optimal conversion rate strategy (Figure 5B). Degrees of freedom, at least for infected RBC-based cue, did not have a significant impact on optimal conversion rate strategy (Figure 5C). Coupling GA with another algorithm such as Nelder-Mead or L-BFGS-B significantly improved optimal fitness calculation (Fig 5E).

Overall, future modelling attempts should continue the use of double exponential transformation and degree of freedom=3. However, we should test out different cue ranges and perform optimization using a hybrid-GA approach.

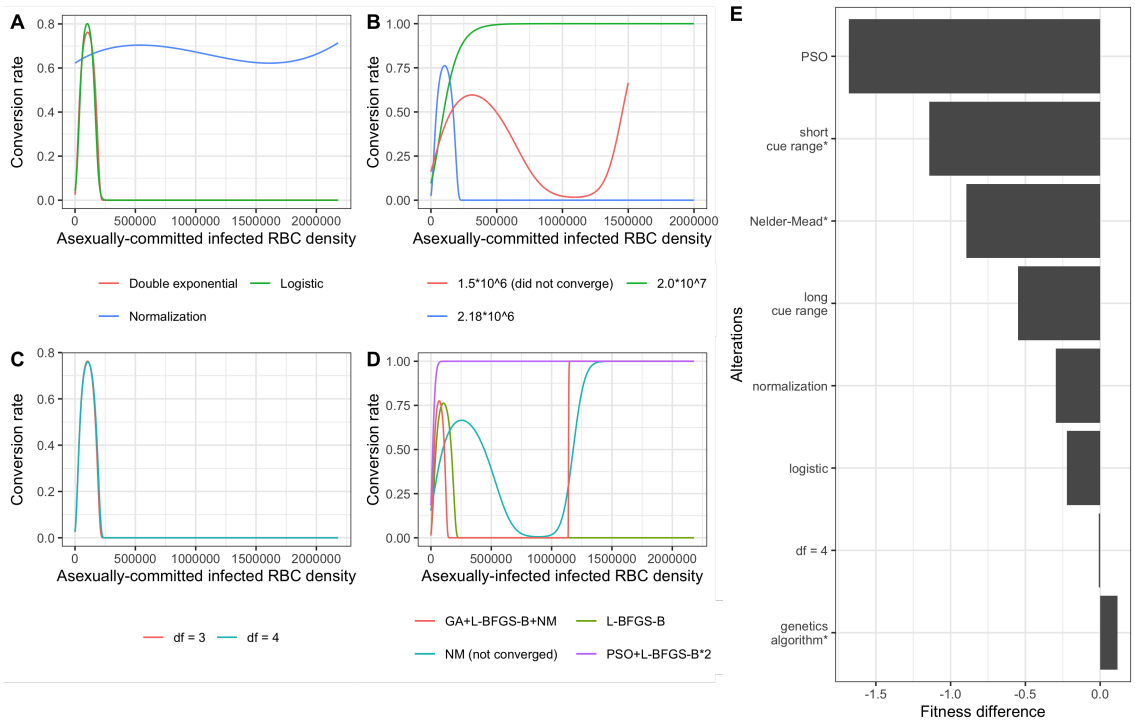

Figure 5: Modelling choices affected optimal conversion rate estimation. (A) Normalizing conversion rate results in suboptimal conversion rate strategy optimization. (B) Long cue range resulted in suboptimal conversion rate strategy optimization while shorter cue range increases chance of non-convergence. (C) Degrees of freedom had little effect on conversion rate strategy optimization. (D) Choice of optimization algorithm significantly affected optimal conversion rate strategy. (E) Fitness difference between models with following alterations compared to the default model (double exponential transformation, $2.18 * 10^6$ cue rane, df = 3, L-BFGS-B optimizer). All infections are simulated assuming saturating immunity. Non-convergence is either stated explicitly or marked by *.

Future tasks

In the past weeks, I was able to build most of the basic tools required to simulate single strain infection. However, many issues remain. The biggest issue perhaps is the consistently high conversion rate strategy predicted by our models that does not abide by our observation that conversion rate tend to be low in typical infections. There are several explanations for the high conversion rate strategy:

- In our models, especially those that adopt a robust mode of innate immunity, there is a lot of advantages to having high conversion rate (lower infected RBC density = less immunity elicited + more gametocyte) and little advantages in investing more energy into producing merozoites (high immunity+little gametocyte).
- Non-inclusion of biological phenomenons that increases the benefit of a low conversion rate, such as co-infection, adaptive immunity, and immunity-removal of gametocyte/merozoite
- Conversion rate is unrestricted (no upper limit).
- Inaccurate measurement of fitness, which includes measurement of fitness itself, the duration of infection, the importance of early infection infectiousness vs late infection infectiousness (currently valued the same) ...

Hence, in the next few days, I will work on the inclusion of:

- adaptive immunity
- co-infection dynamics
- different modes of measuring fitness (without delving into nested model)

Simulating co-infection dynamics will be an especially large challenge, given that the current approach involves manually fixing the best conversion rate strategy and allowing the optimizer to figure out the next best conversion rate strategy. While we can automate this process, the process should also allow for drastic differences in conversion rate strategy, which is also the issue with local optimization methods. I have an idea with using the principles of GA to simulate many two-strategies tournament and select for the strategy that has the average highest fitness. But that remains to be thought out thoroughly.

Appendix

In the original Greischar model, merozoites born from the inoculated asexual infected RBC can immediately produce sexually-committed RBC. However, if we assume that all inoculated infected RBCs are asexually-committed and that all parasites adopt next cycle conversion, we would expect the initial inoculum to produce all asexually-committed merozoite. Hence, the earliest day at which sexually-committed infected RBC can be produced is on day one (α) and the earliest day that gametocyte will emerge is on day three ($\alpha + \alpha_G$). Thus, the lag model can be segregated into four time periods: $t \leq \alpha$, $t > \alpha$, $\alpha < t \leq \alpha + \alpha_G$, and $t > \alpha + \alpha_G$.

When $t \leq \alpha$, only asexually-committed merozoite and infected RBC can be produced (all derive from initial inoculate) such that:

$$\frac{dI}{dt} = pR(t)M(t) - I_0 beta(s_p, s_p)S - \mu I(t) - DI(t)$$

where infected RBC density (I) is increased when asexually-committed merozoite (M) invades susceptible RBC (R) at a probability (p). Asexually-committed infected RBC density decrease when the initial inoculated RBC (I_0) burst, die from natural causes at a rate of μ, or are removed by immunity at a rate of D. Under our assumption, when the initially inoculated infected RBC (I_0) burst, they can only produce β asexually-committed merozoite (M) such that:

$$\frac{dM}{dt} = \beta I_0 beta(s_p, s_p)S - \mu_M M(t) - pR(t)M(t)$$

where asexually-committed merozoite is removed by natural death at a rate of μ_M or when they invade RBC. Given that all the initially innoculated RBC produces only asexually-committed merozoite, there is no production of sexually-committed merozoite (M_G), sexually-committed infected RBC (I_G) or gametocyte (G).

$$\frac{dM_G}{dt} = 0; \frac{dI_G}{dt} = 0; \frac{dG}{dt} = 0$$

Survival of an infected RBC through this period is defined by the natural death rate of RBCs (μ) and immunity action (D).

$$S = e^{-\int_0^t \mu + D\, dw}$$

When $t > \alpha$, the first generation of asexually- (M) and sexually-committed merozoite (M_G) is produced and this phase constitutes the final "stage" of the asexual replication phase such that:

$$\frac{dI}{dt} = pR(t)M(t) - pR(t-\alpha)M(t-\alpha)S - \mu I(t) - DI(t)$$

$$\frac{dM}{dt} = \beta(1 - c(t-\alpha))pR(t-\alpha)M(t-\alpha)S - \mu_M M(t) - pR(t)M(t)$$
$$\frac{dM_G}{dt} = \beta c(t-\alpha)pR(t-\alpha)M(t-\alpha)S - \mu_M M_G(t) - pR(t)M_G(t)$$

where the decision to make asexually-committed/sexually-committed merozoite is made at the beginning of infected RBC development. For part of this period, $\alpha < t \leq \alpha + \alpha_G$, no gametocytes are produced given that none of the sexually-committed RBCs have completed the development period yet such that:

$$\frac{dI_G}{dt} = pR(t)M_G(t) - \mu I_G(t) - DI_G(t)$$

$$\frac{dG}{dt} = 0$$

When $t > \alpha + \alpha_G$, the earliest population of sexually-infected RBC burst to produce gametocyte such that:

$$\frac{dI_G}{dt} = pR(t)M_G(t) - \mu I_G(t) - DI_G(t) - pR(t-\alpha_G)M_G(t-\alpha_G)S_G$$

$$\frac{dG}{dt} = pR(t-\alpha_G)M_G(t-\alpha_G)S_G - \mu_G G(t)$$

where the survival of sexually-commmitted infected RBC (I_G) is represented by:

$$S_G = e^{-\int_{t-\alpha_G}^{t} \mu + D\, dw}$$